Shock and Vibration 11 (2004) 585–596
IOS Press

A high precision shear flexible triangular element for vibration of composite shells

A.H. Sheikh[a,*], S. Haldar[b] and D. Sengupta[b]
[a]*Department of Ocean Engineering and Naval Architecture, Indian Institute of Technology, Kharagpur – 721 302, India*
[b]*Department of Applied Mechanics, Bengal Engineering College* (*Deemed University*), *Howrah – 7111 103, India*

Received 25 April 2003
Revised 2004

Abstract. A high precision triangular shallow shell element is proposed and it is applied to free vibration analysis of composite and isotropic shells. The Mindlin's hypothesis is followed to include the effect of shear deformation. The formulation is made in an efficient manner to make the element free from shear locking problem. The element has some internal nodes, which are eliminated through static condensation technique to improve the computational elegance of the element. In the present vibration problem, the implementation of the static condensation became possible with the help of an efficient mass lumping scheme. It is quite interesting that the effect of rotary inertia can be included in the recommended scheme for lumped mass matrix. Numerical examples covering a wide range of problems are solved and the results obtained are compared with the published results in many cases, which show the precision and range of applicability of the proposed element. The performance of the proposed technique for rotary inertia is found to be excellent. Some new results are produced, which may be useful in future research.

1. Introduction

The finite element method [2,15,28,29] is regarded as the most powerful tool specifically in structural analysis problems. The analysis of plate and shell is one of the first problems where finite element was applied in early sixties of last century. The initial attempts were made with Kirchhoff's hypothesis where a number of problems were faced. The major problem was concerned with the satisfaction of normal slope continuity at the element edges, which could not be solved yet. In the subsequent study, the Mindlin's hypothesis was followed to include the effect of shear deformation where the above mentioned continuity problem could be avoided. This is achieved by considering the transverse displacement (w) and rotations of the normal (θ_x and θ_y) as the independent displacement components. In this group the most popular elements are based on isoparametric formulation. Though these elements are quite elegant but they suffer from certain problems like shear locking, stress extrapolation, spurious modes and something else.

Keeping these aspects in view, some investigations have been carried out to find out some amendments, alternative formulations or some other techniques (e.g. [3,10,13,14,20,27,30]) to achieve an element, which may be applied with improved accuracy without facing the above problems. This is clearly reflected in the recent review papers on shell finite elements [28]. The requirement for the development of such elements has been increased with the popularity of fibre reinforced laminated composites as structural material where the effect of shear deformation is quite significant. Actually composite is weak in shear due to its low shear modulus compared to extensional rigidity. Moreover, the layered configuration in these structures causes further complications. The transverse strains (normal as well as shear) are found to be discontinuous at the layer interfaces, which can be represented by zigzag through

*Corresponding author. Tel.: +91 3222 83790; Fax: +91 3222 55303; E-mail: hamid@naval.iitkgp.ernet.in.

ISSN 1070-9622/04/$17.00

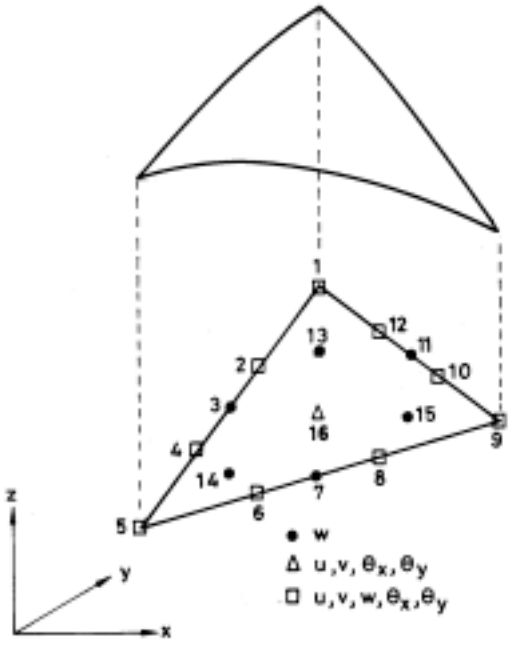

Fig. 1. A typical shell element projected in the base plane.

thickness variation of displacement components [7]. On the other hand, transverse stresses become continuous at the layer interfaces [5,6]. The effect of these refinements in the evaluation of global response parameters like natural frequencies of vibration is not so prominent as that found in the evaluation of stresses specifically transverse stresses [8]. All these have inspired the researchers (e.g. [1,4,5,8,16,21,23–26]) to make this an active area of research in recent days. However, the present study is based on Mindlin's hypothesis in order to have a simple representation of the structural deformation.

In this context, the triangular Mindlin plate element developed by one of the authors (Sengupta [20]) is quite interesting. This trouble free element based on a simple idea is found to give very good results even with a coarse mesh in the static analysis of isotropic plates [20]. It has inspired the authors to develop the proposed shallow shell element using the basic concept of the high precision triangular Mindlin plate element [20]. The performance of the element has been found to be very good in the prediction of structural response under static load [21] while that is tested for the prediction of vibration characteristics in the present study. In the shell element the transverse displacement w is expressed by a complete fourth order polynomial while complete cubic polynomials are used to express the in-plane displacements (u and v) and the rotations (θ_x and θ_y) of the normal. Thus the interpolation function of w is one order higher than that of θ_x and θ_y, which has helped to make this element free from locking and other relevant problems.

The fifty-five unknowns in these five polynomials can be easily expressed in terms of fifty-five nodal displacements of the element as shown in Fig. 1. With this the stiffness and mass matrices of an order of fifty-five can be derived following the usual steps of finite element technique. Though these matrices can be used directly in these forms but their implementation and use will be quite cumbersome due to the presence of the internal nodes. This can be avoided by eliminating the degrees of freedom of the internal nodes. Actually Sengupta [20] has done it using the technique of static condensation, which is quite easy to implement in a static analysis [20]. This is somewhat difficult in the present vibration problem due to the presence of the mass matrix in the governing equation. The problem will be much more severe if a consistent mass matrix is used where the matrix is more populated and having coupling of the degrees of freedom for the internal and external nodes. On the other hand the effect of rotary inertia can easily be incorporated in the formulation with consistent mass matrix. In the present element, the condensation technique of Guyan [11] and something else cannot be applied, as it contributes a significant amount of mass at the internal

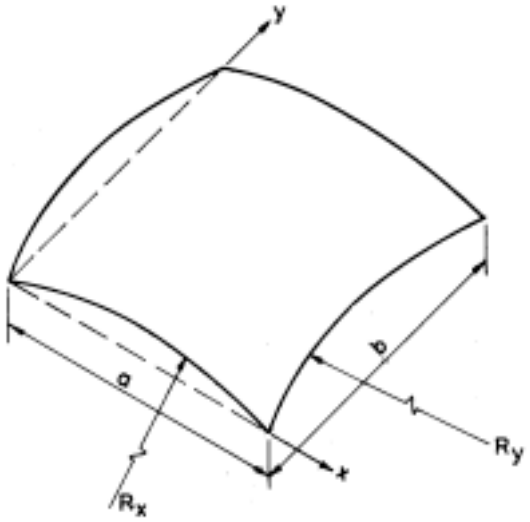

Fig. 2. Geometry and axis system of a doubly curved shell panel.

nodes. In this situation, the only alternative is to have a mass matrix having no mass contribution at the internal nodes. This is achieved with the proposed mass lumping scheme where the mass of an element is distributed at the external nodes only. Interestingly, some recommendation has also been made for the incorporation of rotary inertia in lumped mass matrix. The detail of the lumping scheme is presented in the formulation.

Numerical examples of isotropic and composite shells having different curvature, aspect ratio, boundary condition, number of layers, fibre orientation and thickness ratio (h/a) are solved by the proposed element. A large number of these results are compared with the results available in literature, which clearly reflects the performance of the proposed element.

2. Formulation

The formulation is based on shallow shell theory with the usual assumptions. The effect of shear deformation is taken into account following the Mindlin's hypothesis. The area co-ordinate system [29] is used to do the formulation.

Figure 1 shows a typical shell element projected in the base plane. The locations of the nodes 1, 2, 3, 13 and 16 are (1, 0, 0), (2/3, 1/3, 0), (1/2, 1/2, 0), (1/2, 1/4, 1/4) and (1/3, 1/3, 1/3) respectively. Using symmetry the locations of other nodes can be easily obtained. The degrees of freedom at all the external nodes except 3, 7 and 11 are u, v, w, θ_x and θ_y while it is only w at nodes 3, 7, 11, 13, 14 and 15. Node 16 contains u, v, θ_x and θ_y.

According to earlier discussion the independent displacement components may be expressed as follows

$$u = [Q_3]\{\alpha\}, \tag{1a}$$

$$\nu = [Q_3]\{\beta\} \tag{1b}$$

$$w = [Q_4]\{\gamma\}, \tag{1c}$$

$$\theta_x = [Q_3]\{\mu\} \tag{1d}$$

$$\text{and} \quad \theta_y = [Q_3]\{\lambda\}, \tag{1e}$$

where $[Q_3] = [L_1^3 \;\; L_2^3 \;\; L_3^3 \;\; L_1^2L_2 \;\; L_2^2L_1 \;\; L_2^2L_3 \;\; L_3^2L_2 \;\; L_3^2L_1 \;\; L_1^2L_3 \;\; L_1L_2L_3]$,

$$[Q_4] = [L_1^4 \;\; L_2^4 \;\; L_3^4 \;\; L_1^3L_2 \;\; L_2^3L_1 \;\; L_2^3L_3 \;\; L_3^3L_2 \;\; L_3^3L_1 \;\; L_1^3L_3 \;\; L_1^2L_2^2 \;\; L_2^2L_3^2 \;\; L_3^2L_1^2 \;\; L_1^2L_2L_3 \;\; L_1L_2^2L_3 \;\; L_1L_2L_3^2],$$

Table 1
Frequency parameters ($\omega a^2\sqrt{(\rho h)/D}$) of an isotropic doubly curved shell panel (Fig. 2) clamped at $y = 0$ and free at the other sides ($a/b = 1, a/R_x = 0.2, \nu = 0.3$)

h/a	R_y/R_x	References	Mode number					
			1	2	3	4	5	6
0.01	−2.0	MLS-2[a] (8 × 8[b])	7.490	8.834	29.982	32.965	38.750	56.660
		MLS-2 (10 × 10)	7.492	8.839	30.091	33.089	38.816	56.746
		MLS-2 (12 × 12)	7.492	8.840	30.140	33.111	38.883	56.847
		ISSE9 (14 × 14)	7.414	9.193	30.127	32.981	40.232	57.496
		ISSE9 (16 × 16)	7.440	9.125	30.165	33.026	39.999	57.438
		ISSE9 (18 × 18)	7.458	9.076	30.184	33.060	39.828	57.391
		ISSE9 (20 × 20)	7.471	9.040	30.194	33.085	39.698	57.352
		Leissa et al. [17]	7.507	8.872	30.165	33.180	38.974	57.203
	−1.0	MLS-2 (8 × 8)	6.486	8.764	29.772	32.477	45.829	64.409
		MLS-2 (10 × 10)	6.489	8.769	29.811	32.517	45.912	64.566
		MLS-2 (12 × 12)	6.489	8.770	29.823	32.534	45.933	64.582
		ISSE9 (20 × 20)	6.525	8.911	29.713	33.286	46.448	64.707
		Leissa et al. [17]	6.504	8.802	29.931	32.683	46.125	65.010
	2.0	MLS-2 (8 × 8)	7.751	8.860	24.463	32.528	36.322	65.441
		MLS-2 (10 × 10)	7.752	8.865	24.518	32.581	36.377	65.721
		MLS-2 (12 × 12)	7.752	8.866	24.540	32.598	36.391	65.912
		ISSE9 (20 × 20)	7.745	9.090	24.823	32.296	38.358	64.898
		Leissa et al. [17]	7.765	8.897	24.664	32.777	36.566	66.427
0.1	−2.0	MLS-2 (8 × 8)	3.511	8.031	20.219	20.958	25.377	28.088
		MLS-2 (10 × 10)	3.514	8.037	20.248	20.962	25.429	28.180
		MLS-2 (12 × 12)	3.514	8.040	20.255	20.964	25.467	28.231
		ISSE9 (20 × 20)	3.548	8.108	20.379	21.775	25.743	28.538
	−1.0	MLS-2 (8 × 8)	3.512	7.997	20.240	20.868	25.371	28.350
		MLS-2 (10 × 10)	3.513	8.003	20.269	20.874	25.484	28.394
		MLS-2 (12 × 12)	3.513	8.004	20.280	20.876	25.538	28.412
		ISSE9 (20 × 20)	3.547	8.076	20.391	21.616	25.862	38.687
	2.0	MLS-2 (8 × 8)	3.503	8.037	20.088	20.917	25.438	28.195
		MLS-2 (10 × 10)	3.504	8.043	20.118	20.923	25.491	28.240
		MLS-2 (12 × 12)	3.504	8.045	20.127	20.925	25.506	28.245
		ISSE9 (20 × 20)	3.538	8.113	20.250	21.741	25.802	28.554

[a]analysis based on proposed element using MLS-2 as the mass lumping scheme.
[b]indicates mesh size.

$$\{\alpha\} = [\alpha_1\ \alpha_2\ \alpha_3\ \alpha_4\ \alpha_5\ \alpha_6\ \alpha_7\ \alpha_8\ \alpha_9\ \alpha_{10}]^T,$$
$$\{\beta\} = [\beta_1\ \beta_2\ \beta_3\ \beta_4\ \beta_5\ \beta_6\ \beta_7\ \beta_8\ \beta_9\ \beta_{10}]^T,$$
$$\{\gamma\} = [\gamma_1\ \gamma_2\ \gamma_3\ \gamma_4\ \gamma_5\ \gamma_6\ \gamma_7\ \gamma_8\ \gamma_9\ \gamma_{10}\ \gamma_{11}\ \gamma_{12}\ \gamma_{13}\ \gamma_{14}\ \gamma_{15}]^T,$$
$$\{\mu\} = [\mu_1\ \mu_2\ \mu_3\ \mu_4\ \mu_5\ \mu_6\ \mu_7\ \mu_8\ \mu_9\ \mu_{10}]^T$$
$$\text{and } \{\lambda\} = [\lambda_1\ \lambda_2\ \lambda_3\ \lambda_4\ \lambda_5\ \lambda_6\ \lambda_7\ \lambda_8\ \lambda_9\ \lambda_{10}]^T,$$

The unknowns ($\{\alpha\}, \{\beta\}, \{\gamma\}, \{\mu\}$ and $\{\lambda\}$) in the above Eq. (1) can be expressed in terms of nodal displacements by substitution of these equations at the different nodes appropriately, which leads to

$$\{X\} = [A]\{\delta\} \text{ or } \{\delta\} = [A]^{-1}\{X\}, \tag{2}$$

where $\{\delta\} = \left[[\alpha]^T\ \ [\beta]^T\ \ [\gamma]^T\ \ [\mu]^T\ \ [\lambda]^T\right]^T$,

$$\{X\}^T = [u_1\ \nu_1\ w_1\ \theta_{x1}\ \theta_{y1}\ u_2\ \nu_2\ w_2\ \theta_{x2}\ \theta_{y2}\ w_3\ u_4\ \nu_4\ w_4\ \theta_{x4}\ \theta_{y4}\ u_5\ \nu_5\ w_5\ \theta_{x5}\ \theta_{y5}\ u_6\ \nu_6\ w_6\ \theta_{x6}\theta_{y6}w_7\ u_8$$
$$\nu_8\ w_8\ \theta_{x8}\ \theta_{y8}\ u_9\ \nu_9\ w_9\ \theta_{x9}\ \theta_{y9}\ u_{10}\ \nu_{10}\ w_{10}\ \theta_{x10}\ \theta_{y10}\ w_{11}\ u_{12}\ \nu_{12}\ w_{12}\ \theta_{x12}\ \theta_{y12}\ w_{13}\ w_{14}\ w_{15}$$
$$u_{16}\ \nu_{16}\ \theta_{x16}\ \theta_{y16}]$$

and the matrix $[A]$ having an order of 55 × 55 can be obtained with the co-ordinates of the different nodes.

The generalised stress strain relationship of a laminated shell may be written as

Table 2
Frequency parameters ($100\omega a\sqrt{\rho/E}$) of an isotropic cylindrical shell panel (Fig. 3) simply supported at the four sides ($a/b = 1, a/R = 0.5, \nu = 0.3$)

h/a	Reference	Mode numbers					
		1	2	3	4	5	6
0.1	MLS-1[a] (4 × 4)	74.792	140.31	146.99	216.66	261.14	265.13
	MLS-1 (6 × 6)	74.828	140.54	147.26	217.42	262.59	266.67
	MLS-1 (8 × 8)	74.842	140.62	147.36	217.74	263.15	267.26
	MLS-1 (10 × 10)	74.847	140.66	147.40	217.89	263.42	267.53
	MLS-1 (12 × 12)	74.848	140.68	147.42	217.98	263.51	267.60
	MLS-2 (4 × 4)	74.289	138.20	144.75	212.19	255.08	258.95
	MLS-2 (6 × 6)	74.282	138.40	144.99	212.85	256.32	260.28
	MLS-2 (8 × 8)	74.295	138.48	145.09	213.14	256.82	260.79
	MLS-2 (10 × 10)	74.301	138.51	145.13	213.27	257.04	261.03
	MLS-2 (12 × 12)	74.301	138.52	145.15	213.30	257.25	261.13
	ISSE9 (20 × 20)	74.164	138.13	144.70	212.36	255.64	259.67
	Lim and Liew[b] [18]	74.367	139.05	145.25	213.69	258.11	261.57
	Lim and Liew[c] [18]	74.365	139.02	145.23	213.63	258.01	261.49
0.2	MLS-1 (4 × 4)	117.49	235.64	241.02	340.53	398.24	401.37
	MLS-1 (6 × 6)	117.64	236.78	242.26	343.96	403.91	407.22
	MLS-1 (8 × 8)	117.69	237.19	242.70	345.22	405.97	409.35
	MLS-1 (10 × 10)	117.71	237.38	242.92	345.81	406.94	410.35
	MLS-1 (12 × 12)	117.71	237.45	242.99	346.06	407.67	410.69
	MLS-2 (4 × 4)	115.00	228.27	233.28	329.00	368.99	371.83
	MLS-2 (6 × 6)	115.13	229.24	234.34	331.88	389.59	392.67
	MLS-2 (8 × 8)	115.17	229.59	234.72	332.95	391.33	394.46
	MLS-2 (10 × 10)	115.19	229.76	234.90	333.46	392.16	395.30
	MLS-2 (12 × 12)	115.20	229.89	235.01	334.03	392.41	395.56
	ISSE9 (20 × 20)	114.67	227.90	232.98	329.75	390.19	392.32
	Lim and Liew[b] [18]	115.38	231.34	235.53	335.29	395.85	397.87

[a]Analysis based on proposed element using MLS-1 as the mass lumping scheme.
[b]Results based on higher order shear deformation theory (HSDT).
[c]Results based on first order shear deformation theory (FSDT).

$$\{\sigma\} = [D]\{\varepsilon\}, \tag{3}$$

$$\text{where } \{\sigma\}^T = [N_x \;\; N_y \;\; N_{xy} \;\; M_x \;\; M_y \;\; M_{xy} \;\; Q_x \;\; Q_y], \tag{4}$$

$$\{\varepsilon\} = \begin{Bmatrix} \partial u/\partial x + w/R_x \\ \partial \nu/\partial y + w/R_y \\ \partial u/\partial y + \partial \nu/\partial x + 2w/R_{xy} \\ -\partial \theta_x/\partial x \\ -\partial \theta_y/\partial y \\ -\partial \theta_x/\partial y - \partial \theta_y/\partial x \\ \partial w/\partial x - \theta_x \\ \partial w/\partial y - \theta_y \end{Bmatrix} \tag{5}$$

$$\text{and } [D] = \begin{bmatrix} A_{11} & A_{12} & A_{16} & B_{11} & B_{12} & B_{16} & 0 & 0 \\ A_{21} & A_{22} & A_{26} & B_{21} & B_{22} & B_{26} & 0 & 0 \\ A_{61} & A_{62} & A_{66} & B_{61} & B_{62} & B_{66} & 0 & 0 \\ B_{11} & B_{12} & B_{16} & D_{11} & D_{12} & D_{16} & 0 & 0 \\ B_{21} & B_{22} & B_{26} & D_{21} & D_{22} & D_{26} & 0 & 0 \\ B_{61} & B_{62} & B_{66} & D_{61} & D_{62} & D_{66} & 0 & 0 \\ 0 & 0 & 0 & 0 & 0 & 0 & A_{55} & A_{54} \\ 0 & 0 & 0 & 0 & 0 & 0 & A_{45} & A_{44} \end{bmatrix} \tag{6}$$

Table 3
Frequency parameters ($\omega a^2\sqrt{\rho/E_2h^2}$) of a cross-ply spherical shell panel (Fig. 2) simply supported at the four sides ($a/b = 1, E_1/E_2 = 25, G_{12} = G_{13} = 0.5E2, G_{23} = 0.2E_2, \nu_{12} = 0.25$)

R_x/a	References	Mode numbers					
		1	2	3	4	5	6
		Two layer (0/90)					
3	MLS-2 (8 × 8)	9.8531	21.425	21.425	21.736	22.005	29.702
	MLS-2 (10 × 10)	9.8546	21.427	21.427	21.752	22.021	29.742
	MLS-2 (12 × 12)	9.8551	21.428	21.428	21.760	22.030	29.750
	ISSE9 (20 × 20)	9.8288	21.596	21.868	22.141	22.155	29.453
	Reddy [19]	9.9608					
5	MLS-2 (8 × 8)	9.2555	21.425	21.425	21.453	21.619	29.541
	MLS-2 (10 × 10)	9.2567	21.427	21.427	21.468	21.635	29.581
	MLS-2 (12 × 12)	9.2572	21.428	21.428	21.473	21.641	29.592
	ISSE9 (20 × 20)	9.2502	21.314	21.484	22.141	22.155	29.296
	Reddy [19]	9.2309					
10	MLS-2 (8 × 8)	8.9865	21.350	21.425	21.425	21.434	29.454
	MLS-2 (10 × 10)	8.9876	21.365	21.427	21.427	21.449	29.494
	MLS-2 (12 × 12)	8.9881	21.371	21.427	21.427	21.455	29.504
	ISSE9 (20 × 20)	8.9839	21.211	21.230	22.141	22.156	29.230
	Reddy [19]	8.9841					
		Four layer (0/90/90/0)					
3	MLS-2 (8 × 8)	12.893	22.210	22.210	22.684	29.695	35.079
	MLS-2 (10 × 10)	12.897	22.211	22.212	22.702	29.736	35.147
	MLS-2 (12 × 12)	12.900	22.211	22.212	22.710	29.751	35.168
	ISSE9 (20 × 20)	12.876	22.174	22.193	22.509	29.242	34.638
	Reddy [19]	12.795					
5	MLS-2 (8 × 8)	12.469	21.427	21.427	22.345	29.478	34.951
	MLS-2 (10 × 10)	12.472	21.429	21.429	22.363	29.519	35.018
	MLS-2 (12 × 12)	12.473	21.429	21.429	22.368	29.528	35.032
	ISSE9 (20 × 20)	12.451	22.174	22.181	22.192	29.039	34.514
	Reddy [19]	12.437					
10	MLS-2 (8 × 8)	12.283	21.427	21.427	22.203	29.391	34.897
	MLS-2 (10 × 10)	12.285	21.429	21.429	22.220	29.432	34.964
	MLS-2 (12 × 12)	12.285	21.429	21.429	22.225	29.442	34.987
	ISSE9 (20 × 20)	12.214	22.040	22.174	22.192	28.952	34.462
	Reddy [19]	12.280					

The rigidity matrix $[D]$ constitutes of the contributions of its individual layers. Using the material properties and fiber orientation of the individual layers it can be easily obtained following the steps available in any standard text on mechanics of fiber reinforced laminated composites. For the evaluation of rigidity parameters for transverse shear (A_{44}, A_{45}, A_{54} and A_{55}), a shear correction factor of 5/6 is used.

Now the field variables as expressed in Eq. (1) may be substituted in Eq. (5) to express the strain vector $\{\varepsilon\}$ as

$$\{\varepsilon\} = [C]\{\delta\}. \tag{7}$$

With the help of Eq. (2) the strain vector $\{\varepsilon\}$ in Eq. (7) may be expressed in terms of nodal displacement vector $\{X\}$ as

$$\{\varepsilon\} = [C][A]^{-1}\{X\} = [B]\{X\}. \tag{8}$$

Once the matrices $[B]$ and $[D]$ are obtained, the element stiffness matrix $[K_e]$ can be easily derived using the help of Virtual work technique and it may be expressed as

$$[K_e] = \int_A [B]^T[D][B]dxdy \tag{9}$$

In a similar manner the consistent mass matrix of an element can be derived with the help of the Eqs (1) and (2) and it may be expressed as

Table 4
Frequency parameters ($\omega a^2\sqrt{\rho/E_2h^2}$) of a cross-ply (0/90/0) cylindrical shell panel (Fig. 3) simply supported at the four sides ($a/b = 1, E_1/E_2 = 25, G_{12} = G_{13} = 0.5E_2, G_{23} = 0.5E_2, \nu_{12} = 0.25$)

R/a	References	Mode numbers					
		1	2	3	4	5	6
		$h/a = 0.01$					
4	MLS-2 (8 × 8)	22.708	40.221	56.717	61.727	62.501	75.124
	MLS-2 (10 × 10)	22.708	40.221	56.719	61.728	62.502	75.120
	MLS-2 (12 × 12)	22.708	40.221	56.720	61.728	62.502	75.119
	ISSE9 (20 × 20)	22.705	40.218	56.691	61.712	62.477	75.080
	Reddy [19]	22.709					
5	MLS-2 (8 × 8)	20.333	35.002	55.005	56.666	61.822	73.741
	MLS-2 (10 × 10)	20.333	35.002	55.005	56.668	61.823	73.736
	MLS-2 (12 × 12)	20.333	35.002	55.005	56.668	61.823	73.735
	ISSE9 (20 × 20)	20.325	34.985	54.952	56.506	61.661	73.542
	Reddy [19]	20.332					
10	MLS-2 (8 × 8)	16.625	26.400	44.329	56.284	60.576	70.310
	MLS-2 (10 × 10)	16.625	26.400	44.330	56.287	60.578	70.310
	MLS-2 (12 × 12)	16.625	26.400	44.330	56.288	60.579	70.310
	ISSE9 (20 × 20)	16.620	26.398	44.320	56.257	60.553	70.279
	Reddy [19]	16.625					
		$h/a = 0.1$					
4	MLS-2 (8 × 8)	12.232	18.934	21.427	21.427	30.844	31.079
	MLS-2 (10 × 10)	12.235	18.945	21.429	21.429	30.891	31.125
	MLS-2 (12 × 12)	12.236	18.949	21.430	21.430	30.912	31.132
	ISSE9 (20 × 20)	12.166	18.845	22.178	22.183	30.245	30.879
	Reddy [19]	12.233					
5	MLS-2 (8 × 8)	12.204	18.851	21.427	21.427	30.849	30.980
	MLS-2 (10 × 10)	12.207	18.861	21.429	21.429	30.894	31.026
	MLS-2 (12 × 12)	12.208	18.854	21.430	21.430	30.917	31.035
	ISSE9 (20 × 20)	12.137	18.761	22.178	22.183	30.250	30.781
	Reddy [19]	12.207					
10	MLS-2 (8 × 8)	12.167	18.738	21.427	21.427	30.848	30.857
	MLS-2 (10 × 10)	12.170	18.748	21.429	21.429	30.894	30.904
	MLS-2 (12 × 12)	12.171	18.751	21.430	21.430	30.918	30.918
	ISSE9 (20 × 20)	12.099	18.649	22.178	22.183	30.256	30.649
	Reddy [19]	12.173					

$$[M_e] = [A]^{-T}\rho h \int_A \begin{pmatrix} [Q_u]^T[Q_u] + [Q_v]^T[Q_v] + [Q_w]^T[Q_w] \\ +\frac{h^2}{12}[Q_{\theta x}]^T[Q_{\theta x}] + \frac{h^2}{12}[Q_{\theta y}]^T[Q_{\theta y}] \end{pmatrix} dxdy[A]^{-1}, \tag{10}$$

where $[Q_u] = [[Q_3][N_1][N_2][N_1][N_1]], [Q_v] = [[N_1][Q_3][N_2][N_1][N_1], [Q_w] = [[N_1][N_1[Q_4][N_1][N_1]]$,
$[Q_{\nu x}] = [[N_1][N_1][N_2][Q_3][N_1]]$
and $[Q_{\nu y}] = [[N_1][N_1][N_2][N_1][Q_3]]$.

In the above equation $[N_1]$ and $[N_2]$ are null matrices of order 1×10 and 1×15 respectively. The first three terms of the mass matrix in Eq. (10) are associated with the movement of mass along u, ν and w respectively, which are found to contribute the major inertia. The last two terms are associated with rotary inertia and their contribution is expected to be significant in thick shell only. The integration found in Eqs (9) and (10) is carried out numerically [30] to evaluate the element stiffness and mass matrices.

Though the consistent mass matrix presented in Eq. (10) includes all the contributions including rotary inertia but the difficulty of its use in this form is discussed earlier. It has also been mentioned that the difficulty can be overcome by using a lumped mass matrix based on the mass lumping scheme presented below. In this context two similar mass lumping schemes are proposed where the effect of rotary inertia is taken into account in one case.

In the first lumping scheme (MLS-1), the mass of an element m_e is distributed at w of its external nodes where the ratio of distribution is dependent on the corresponding diagonal elements of the consistent mass matrix $[M_e]$ presented in Eq. (10). This is similarly done for u, v and it is as follows

Table 5
Frequency parameters ($\omega a^2\sqrt{\rho/E_2h^2}$) of an angle-ply (30/-30/...) cylindrical shell panel (Fig. 3) simply supported at the four sides ($a/b = 1, E_1/E_2 = 40$, $G_{12} = G_{13} = G_{23} = 0.5E_2$, $\nu_{12} = 0.25$)

ϕ	References	Mode numbers					
		1	2	3	4	5	6
		30/-30					
20°	MLS-2 (8 × 8)	19.951	29.841	39.186	46.478	53.989	68.040
	MLS-2 (10 × 10)	19.953	29.848	39.203	46.485	54.031	68.124
	MLS-2 (12 × 12)	19.953	29.849	39.210	46.487	54.041	68.145
	ISSE9 (20 × 20)	19.966	29.864	39.239	46.553	54.116	68.366
	Soldatos [22]	18.80					
30°	MLS-2 (8 × 8)	23.315	30.649	40.622	46.898	54.993	68.217
	MLS-2 (10 × 10)	23.318	30.657	40.640	46.926	55.037	68.300
	MLS-2 (12 × 12)	23.318	30.660	40.648	46.935	55.045	68.321
	ISSE9 (20 × 20)	23.325	30.673	40.677	46.994	55.124	68.544
	Soldatos [22]	23.52					
45°	MLS-2 (8 × 8)	29.082	32.460	43.392	47.965	57.078	68.602
	MLS-2 (10 × 10)	29.089	32.468	43.415	47.994	57.075	68.692
	MLS-2 (12 × 12)	29.090	32.471	43.422	48.003	57.075	68.710
	ISSE9 (20 × 20)	29.110	32.489	43.463	48.066	57.175	68.941
	Soldatos [22]	31.36					
		30/-30/30/-30					
20°	MLS-2 (8 × 8)	24.156	38.792	51.624	59.023	70.005	84.455
	MLS-2 (10 × 10)	24.159	38.807	51.662	59.078	70.100	84.616
	MLS-2 (12 × 12)	24.160	38.812	51.675	59.096	70.138	84.721
	ISSE9 (20 × 20)	24.173	38.840	51.736	59.200	70.276	85.012
	Soldatos [22]	24.16					
30°	MLS-2 (8 × 8)	27.270	40.037	52.516	59.455	69.855	84.580
	MLS-2 (10 × 10)	27.275	40.039	52.556	59.512	69.953	84.742
	MLS-2 (12 × 12)	27.277	40.039	52.568	59.536	70.021	84.901
	ISSE9 (20 × 20)	27.285	40.087	52.633	59.635	70.134	85.137
	Soldatos [22]	27.99					
45°	MLS-2 (8 × 8)	32.921	42.562	54.379	60.395	72.640	84.855
	MLS-2 (10 × 10)	32.929	42.583	54.424	60.454	72.747	85.017
	MLS-2 (12 × 12)	32.933	42.588	54.443	60.471	72.789	85.102
	ISSE9 (20 × 20)	32.954	42.626	54.510	60.582	72.944	85.415
	Soldatos [22]	34.84					

$$m_{i,i}^{wl} = \frac{m_{i,i}}{\sum m_{i,i}} m_e \;\; (i = 3, 8, 11, 14, 19, 24, 27, 30, 35, 40, 43, 46) \tag{11a}$$

$$m_{i,i}^{ul} = \frac{m_{i,i}}{\sum m_{i,i}} m_e \;\; (i = 1, 6, 12, 17, 22, 28, 33, 38, 44) \tag{11b}$$

$$\text{and} \;\; m_{i,i}^{vl} = \frac{m_{i,i}}{\sum m_{i,i}} m_e \;\; (i = 2, 7, 13, 18, 23, 29, 34, 39, 45) \tag{11c}$$

where $m_{i,i}^{ul}, m_{i,i}^{vl}$ and $m_{i,i}^{wl}$ are the ith diagonal elements corresponding to u, v and w of the proposed lumped mass matrix $[M_l]$ and $m_{i,i}$ is the ith diagonal element of the consistent mass matrix $[M_e]$.

In the second lumping scheme (MLS-2), the effect of rotary inertia is considered in addition to those ($m_{i,i}^{ul}, m_{i,i}^{vl}$, and $m_{i,i}^{wl}$) taken in the previous case (MLS-1). These additional mass contributions are taken in the following manner

$$m_{i,i}^{\theta xl} = \frac{h^2}{12}\frac{m_{i,i}}{\sum m_{i,i}} m_e \;\; (i = 4, 9, 15, 20, 25, 31, 36, 41, 47) \tag{11d}$$

$$\text{and} \;\; m_{i,i}^{\theta yl} = \frac{h^2}{12}\frac{m_{i,i}}{\sum m_{i,i}} m_e \;\; (i = 5, 10, 16, 21, 26, 32, 37, 42, 48) \tag{11e}$$

Table 6
Frequency parameters ($\omega a^2\sqrt{\rho/E_2h^2}$) of an angle-ply (45/-45/45) spherical shell panel (Fig. 2) having different boundary conditions at the four sides ($R_x/a = 3.0, a/b = 1, E_1/E_2 = 25, G_{12} = G_{13} = 0.5E_2, G_{23} = 0.2E_2, \nu_{12} = 0.25$)

Boundary conditions	References	Mode numbers					
		1	2	3	4	5	6
		$h/a = 0.1$					
C-F-F-F[a]	MLS-2 (8 × 8)	1.8189	5.2302	8.6923	11.380	13.668	16.516
	MLS-2 (10 × 10)	1.8185	5.2347	8.7086	11.385	13.665	16.554
	MLS-2 (12 × 12)	1.8184	5.2355	8.7101	11.386	13.665	16.567
	ISSE9 (20 × 20)	1.8154	5.2411	8.7361	11.374	13.633	16.621
S-S-F-F	MLS-2 (8 × 8)	5.0182	8.3933	17.034	19.007	24.426	27.821
	MLS-2 (10 × 10)	5.0202	8.4017	17.065	19.034	24.484	27.892
	MLS-2 (12 × 12)	5.0213	8.4056	17.076	19.042	24.501	27.913
	ISSE9 (20 × 20)	5.1040	8.4172	17.118	19.085	24.591	28.024
S-S-S-S	MLS-2 (8 × 8)	17.622	23.368	28.839	31.408	34.399	40.297
	MLS-2 (10 × 10)	17.628	23.381	28.875	31.411	34.462	40.401
	MLS-2 (12 × 12)	17.630	23.393	28.891	31.412	34.482	40.467
	ISSE9 (20 × 20)	17.639	23.419	30.980	32.412	34.585	39.604
C-C-C-C	MLS-2 (8 × 8)	21.827	28.321	31.494	37.619	41.951	45.920
	MLS-2 (10 × 10)	21.844	28.358	31.545	37.705	42.070	46.078
	MLS-2 (12 × 12)	21.859	28.373	31.567	37.761	42.105	46.101
	ISSE9 (20 × 20)	21.874	28.425	31.638	37.865	42.299	46.377
		$h/a = 0.2$					
C-F-F-F	MLS-2 (8 × 8)	1.5516	4.1169	6.1968	6.5954	9.4154	11.239
	MLS-2 (10 × 10)	1.5513	4.1195	6.1915	6.6033	9.4257	11.256
	MLS-2 (12 × 12)	1.5513	4.1211	6.1903	6.6061	9.4201	11.269
	ISSE9 (20 × 20)	1.5492	4.1235	6.1658	6.6144	9.4413	11.279
S-S-F-F	MLS-2 (8 × 8)	4.0419	6.8216	12.594	13.011	14.667	15.667
	MLS-2 (10 × 10)	4.0437	6.8283	12.619	13.030	14.670	15.704
	MLS-2 (12 × 12)	4.0445	6.8299	12.627	13.041	14.671	15.616
	ISSE9 (20 × 20)	4.0468	6.802	12.662	13.065	15.708	15.772
S-S-S-S	MLS-2 (8 × 8)	11.002	15.359	15.704	17.255	21.379	23.775
	MLS-2 (10 × 10)	11.009	15.382	15.705	17.288	21.442	23.859
	MLS-2 (12 × 12)	11.012	15.392	15.705	17.302	21.563	23.905
	ISSE9 (20 × 20)	11.023	15.423	15.708	17.345	21.556	24.020
C-C-C-C	MLS-2 (8 × 8)	12.549	16.743	18.014	22.036	24.014	25.314
	MLS-2 (10 × 10)	12.562	16.772	18.051	22.104	24.098	25.423
	MLS-2 (12 × 12)	12.595	16.785	18.063	22.117	24.127	25.487
	ISSE9 (20 × 20)	12.584	16.826	18.119	22.230	24.263	25.620

[a]Clamped at $x = 0$, free at $x = a$, free at $y = 0$ and free at $y = b$.

where the use of $(h^2/12)$ can be justified with the expression of the consistent mass matrix as presented in Eq. (10).

With this lumped mass matrix $[M_l]$ based on MLS-1 or MLS-2, the degrees of freedom of the internal nodes can be condensed out to get the final form of stiffness and mass matrices of an order forty-eight. These matrices are computed for all the elements and assembled together to form the stiffness and mass matrices of the whole structure and these are stored in a single array following the skyline storage technique. The overall system of equations is solved by the simultaneous iterative technique of Corr and Jennings [9] after substitution of boundary conditions, which gives first few frequencies for the lower modes as required.

3. Results and discussions

Numerical examples of isotropic and composite shells are solved by the proposed element to make the validation and study its performance. Problems of isotropic shells are taken, as the element has not been applied to such problems so far. The results obtained in the form of natural frequency for first few modes are presented in non-dimensional form and compared with the published results in many cases. In the absence of suitable published

results, the structure is analysed with an existing shear deformable element to compare the results obtained by the proposed element. In this context a separate computer program (ISSE9) based on nine noded isoparametric element is written where the assumptions are identical to those used in the proposed element.

3.1. Isotropic doubly curved shell

A cantilevered doubly curved shell panel as shown in Fig. 2 (clamped at $y = 0$) is analysed for three different values of R_y/R_x (-2.0, -1.0 and 2.0) taking $h/a = 0.01$ and 0.1. The analysis is carried out by the proposed element with three different mesh divisions taking MLS-2 as the mass lumping scheme. The first six natural frequencies obtained by the proposed element are presented in Table 1 with the analytical solution of Leissa et al. [17]. As the effect of shear deformation and rotary inertia is not considered by Leissa et al. [17], the structure is also analysed by the isoparametric element (ISSE9) and the results obtained are included in Table 1. The results indicate the performance of the proposed element in doubly curved shell panel having complex geometry. In one case ($h/a = 0.01$ and $R_y/R_x = -2$) the analysis with the isoparametric element is carried out with four different mesh sizes (see Table 1). It shows that the isoparametric element requires higher mesh size compared to the proposed element to attain the convergence or to get the desirable accuracy. This infers that the proposed element possesses improved performance compared to isoparametric element. This feature has been highlighted in details by Sengupta [20] with his plate element based on similar concept. For the isoparametric element, a mesh size of 20x20 appears to be sufficient and it is used in the other cases. This is also followed in the subsequent examples where it is used.

3.2. Isotropic cylindrical shell

A cylindrical shell panel as shown in Fig. 3, is analysed by the proposed element with five different mesh divisions taking simply supported boundary condition at the four sides. Using both the mass lumping schemes (MLS-1 and MLS-2) the analysis is carried out for thickness ratio (h/a) of 0.1 and 0.2. The first six natural frequencies obtained in the present analysis are presented in Table 2 with those of Lim and Liew [18] who have solved the problem analytically using higher order shear deformation theory (HSDT). They [18] have also presented some results based on Mindlin's hypothesis i.e., first order shear deformation theory (FSDT). Table 2 shows the performance of the proposed element in terms of convergance rate and solution accuracy. It also indicates that lumping scheme MLS-2 has performed better particularly in the case of higher thickness ratio and it is expected as discussed earlier. This has been throughly studied by Haldar [12] taking different types of plate and shell problems. Based on these observations, MLS-2 may be recommended for the analysis of shell of any thickness while MLS-1 may be used when thickness ratio is reasonable small.

3.3. Cross-ply spherical shell

A cross-ply spherical shell panel on square base simply supported at the four sides is analysed with the proposed element (mesh size: 8×8, 10×10 and 12) taking MLS-2 as mass lumping scheme. The study is made for unsymmetrical (0/90) and symmetrical (0/90/90/0) ply arrangements taking curvature ratio $R_x/a = R_y/b = 3, 5$ and 10 (Fig. 2). In all the cases the thickness ratio (h/a) is taken as 0.1. The first six natural frequencies obtained by the proposed element are presented in Table 3 with the fundamental frequency of Reddy [19] obtained analytically. To compare the results for higher modes the problem is also solved by the isoparametric element and the frequencies obtained are included in Table 3. The table shows that the results obtained from different sources agreed well.

3.4. Cross-ply cylindrical shell

A cross-ply (0/90/0) cylindrical shell panel simply supported at the four sides is analysed for $R_x/a = 4, 5$ and 10 (Fig. 3) taking $h/a = 0.01$ and 0.1. Similar to the previous example the analyis is carried out with the proposed element (mesh size: of 8×8, 10×10 and 12×12) using mass lumping scheme MLS-2 and the isoparametric element (mesh size: 20×20). This analysis scheme is followed in the solution of the problems in the subsequest examples. The first six natural frequencies obtained by both the elements are presented with the fundamental frequency of Reddy [19] in Table 4, which shows that the results agreed well. The material properties and other data are given in Table 4, which is done in the other tables also.

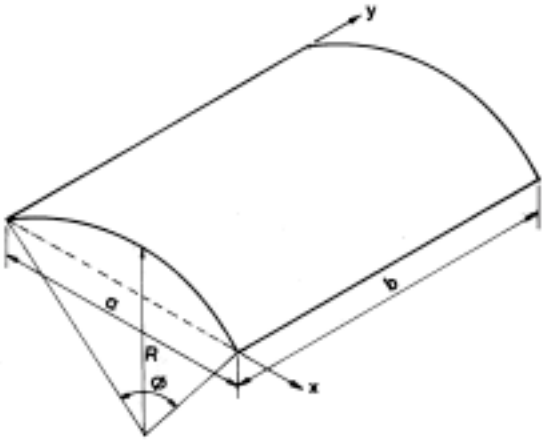

Fig. 3. Geometry and axis system of a cylindrical shell panel.

3.5. Angle-ply cylindrical shell

An angle-ply (30/-30/...) cylindrical shell panel simply supported at the four sides is analysed for the subtended angle $\phi = 20°$, 30° and 45° (Fig. 3) taking $h/a = 0.05$. The analysis is done for two layer (30/-30) and four layer (30/-30/30/-30) ply arrangements using the proposed element and the isoparametric element. The first six natural frequencies obtained by these elements are presented with the fundamental frequency of Soldatos [22] in Table 5. It shows that the results obtained by the proposed element are close to those obtained from other means.

3.6. Angle-ply spherical shell

An angle-ply (45/-45/45) spherical shell panel having a square base is analysed by the proposed element and the isoparametric element taking $R_x/a = R_y/b = 3$ (Fig. 2) and $h/a = 0.1$ and 0.2. The study is made for different combination of boundary conditions at the four sides, which include simply supported, clamped and free edges. The first six natural frequencies obtained in the present analysis are presented in Table 6, which shows that the agreement between the results obtained by the two elements is good.

4. Conclusions

A high precision triangular shallow shell element is proposed. The effect of shear deformation is incorporated in the formulation and it is done in such a manner, which has made the element free from locking in shear. This is based on the concept used in a shear deformable plate element developed by one of the authors of this paper. An effective use of the element in vibration analysis is due the mass lumping scheme proposed in this study. This may be considered as one of the contributions of this paper, as it can be used in any dynamic analysis with an element having internal nodes. The element is applied to the analysis of isotropic and composite shells having different geometry, thickness ratio, stacking sequence, boundary condition and some similar features. The results obtained by the proposed element are compared with the results obtained from other sources, which shows the performance of the element in terms of accuracy and range of applicability. A number of new results particularly for the composite shells are generated. It is expected that these new results will be useful in future research.

References

[1] A. Barut, E. Madenci and A. Tessler, Nonlinear analysis of laminates through a Mindlin type shallow shell element, *Computer Methods in Applied Mechanics and Engineering* **143** (1997), 155–173.
[2] K.J. Bathe, *Finite element procedure*, Prentice-Hall, Englewood Cliffs, New Jersey, 1995.
[3] K.J. Bathe, A. Iosilevich and D. Chapelle, An evaluation of the MITC shell elements, *Computers and Structures* **75** (2000), 1–30.
[4] B. Brank and E. Carrera, A family of shear-deformable shell finite elements for composite structures, *Computers and Structures* **76** (2000), 287–297.
[5] B. Brank and E. Carrera, Multilayered shell finite element with interlaminar continuous shear stresses: a refinement of the Reissner-Mindlin formulation, *International Journal for Numerical Methods in Engineering* **38** (2000), 843–874.
[6] E. Carrera, A study of transverse normal stress effects on vibration of multilayered plates and shells, *Journal of Sound and Vibration* **225** (1999), 803–829.
[7] E. Carrera, Historical review of zig-zag theory for multilayered plates and shells, *Applied Mechanics Review* **56** (2003), 287–308.
[8] E. Carrera, Theories and finite elements for multilayered plates and shells: a unified compact formulation with numerical assessment and benchmarking, *Arch Comp Meth Eng* **10** (2003), 215–296.
[9] R.B. Corr and A. Jennings, A simultaneous iteration algorithm for symmetric eigenvalue problems, *International Journal for Numerical Methods in Engineering* **10** (1976), 647–663.
[10] E.N. Dvorkin and K.J. Bathe, A continuum mechanics based four node shell element for general nonlinear analysis, *Engineering Computations* **1** (1984), 77–88.
[11] R.J. Guyan, Reduction of stiffness and mass matrices, *AIAA Journal* **3** (1965), 380–387.
[12] S. Haldar, *A high precision triangular element with shear deformation for static and dynamic analysis of composite plates, shells and folded plates*, PhD Thesis, Department of Applied Mechanics, Bengal Engineering College, Deemed University, India, 2001.
[13] H.C. Huang and E. Hinton, A nine node Lagrangian Mindlin plate element with enhanced shear interpolation, *Engineering Computations* **1** (1984), 369–379.
[14] T.J.R. Hughes, M. Cohen and M. Haroun, Reduced and selective integration techniques in the finite element analysis of plates, *Nuclear Engineering and Design* **46** (1978), 203–222.
[15] H. Kardestuncer and D.H. Norrie, *Finite element handbook*, McGraw-Hill, New York, 1987.
[16] S. Klinkel, F. Gruttmann and W. Wagner, A continuum based 3D shell element for laminated structures, *Computers and Structures* **71** (1999), 43–62.
[17] A.W. Leissa, J.K. Lee and A.J. Wang, Vibration of cantilevered doubly-curved Shallow shells, *International Journal of Solids Structures* **19** (1983), 411–424.
[18] C.W. Lim and K.M. Liew, A higher order theory for vibration of shear deformable cylindrical shallow shells, *International Journal of Mechanical Sciences* **37** (1995), 277–295.
[19] J.N. Reddy, Exact solutions of moderately thick laminated shells, *Journal of Engineering Mechanics Division, ASCE* **110** (1984), 794–809.
[20] D. Sengupta, Stress analysis of flat plates with shear using explicit stiffness matrix, *International Journal for Numerical Methods in Engineering* **32** (1991), 1389–1409.
[21] A.H. Sheikh, S. Haldar and D. Sengupta, A high precision shell element with shear deformation for the analysis of isotropic and composite shells, *International Journal of Computational Engineering Science* **3** (2002), 277–290.
[22] K.P. Soldatos, Influence of thickness shear deformation on free vibrations of rectangular plates, cylindrical panels and cylinders of antisymmetric angle ply construction, *Journal of sound and vibration* **119** (1987), 111–137.
[23] R.M. Sorem and K.S. Surana, p-version curved shell element for geometrically nonlinear analysis of laminated composite plates and shells, ASME Energy Engineering I, *Composite Materials Design and Analysis* **3** (1997), 85–93.
[24] K.S. Surana, R.M. Sorem and R. Bhatacharya, A survey of theories and finite element formulations for laminated composites, *ASME Composite Materials Design and Analysis* **1** (1996), 179–195.
[25] K.Y. Sze, L.Q. Yao and T.H.H. Pian, An eighteen-node hybrid-stress solid-shell element for homogeneous and laminated structures, *Finite Elements in Analysis and Design* **38** (2002), 353–374.
[26] C.W.S. To and B. Wang, Hybrid strain-based three-node flat triangular laminated composite shell elements for vibration analysis, *Journal of Sound and Vibration* **211** (1998), 277–291.
[27] M.H. Verwood and A.W.M. Kok, A shear locking free six-node Mindlin plate bending element, *Computers and Structures* **36** (1990), 547–555.
[28] H.T.Y. Yang, S. Saigal, A. Masud and R.K. Kapania, A survey of recent shell finite elements, *International Journal for Numerical Methods in Engineering* **47** (2000), 101–127.
[29] O.C. Zienkiewics and R.L. Taylor, *Finite element method: Vol. 2, Solid mechanics*, McGraw-Hill, New York, 2000.
[30] O.C. Zienkiewicz, R.L. Taylor and J.M. Too, Reduce integration technique in general analysis of plates and shells, *International Journal for Numerical Methods in Engineering* **3** (1971), 275–290.